

1 **Title**

2 Modulation of *Sost* gene expression under hypoxia in 3D scaffold-free osteocytic tissue

3

4 **Authors**

5 Jeonghyun Kim and Taiji Adachi

6

7 **Author information**

8 Jeonghyun Kim, PhD

9 Institute for Frontier Life and Medical Sciences, Kyoto University, Kyoto 606-8507, Japan

10 E-mail address: kim.jeonghyun.5m@kyoto-u.ac.jp

11 Tel: +81 75 751 4854

12

13 Taiji Adachi, PhD (Corresponding author)

14 Institute for Frontier Life and Medical Sciences, Kyoto University, Kyoto 606-8507, Japan

15 E-mail address: adachi@infront.kyoto-u.ac.jp

16 Tel: +81 75 751 4853

17

18

19 **Abstract**

20 Bone-related studies have been widely carried out by culturing cells on two-dimensional (2D)
21 culture system due to its easiness of handling, but these 2D *in vitro* achievements may imply a
22 distinct outcome compared to the *in vivo* situation. On the other hand, three-dimensional (3D)
23 culture system has been suggested as a better biomimetic *in vitro* model by providing an
24 appropriate cell-cell or cell-matrix interaction. In this study, we successfully reconstructed a
25 3D disk type of scaffold-free tissue (SFT) using mouse osteoblast-like cells, which evoked an
26 osteocyte differentiation within 2 days. Particularly, the SFT was also utilized as an *in vitro*
27 osteocytic model to elucidate the effect of hypoxia on cellular differentiation capability. As a
28 result, the hypoxia up-regulated a matured osteocyte marker, *Sost*, in the SFT, whereas both
29 osteoblast and osteocyte markers were significantly down-regulated by hypoxia in the 2D
30 conventional monolayer model. The results imply that the hypoxia may enhance the initiation
31 of osteocyte differentiation and retain the osteocyte differentiation in the 3D culture system.
32 Notably, we reported the significance of 3D culture system which might represent the *in vivo*
33 situation regarding cellular response to stimuli. Hence, our study suggests wide applications
34 of SFT using osteoblast cells as a novel *in vitro* osteocyte model for the osteocyte-related
35 studies.

36

37 **Impact statement**

38 In this study, we fabricated a 3D disk type of scaffold-free osteocytic tissue, termed scaffold-
39 free tissue (SFT), reconstructed by mouse osteoblast-like cells. It induced an osteocyte
40 differentiation of osteoblast-like cells in the SFT within 2 days. Moreover, we first showed that
41 a matured osteocyte marker, *Sost*, was modulated by hypoxia in the SFT in a different manner

42 compared to the 2D monolayer. These results highlighted the significance of 3D culture system
43 which might represent the *in vivo* situation regarding cellular response to stimuli. Notably, our
44 model can be utilized as a new *in vitro* osteocyte model for the osteocyte-related studies.

45

46 **Introduction**

47 Osteocytes refer to as bone cells embedded inside the mineralized bone matrix, comprising
48 more than 90% of the bone tissue. The osteocytes are responsible for sensing mechanical
49 stimuli and transducing biochemical signals to osteoclasts for bone resorption and osteoblasts
50 for bone formation^{1,2}. While the mechanical stimuli have been considered as an important
51 factor for cellular behaviors and functions³⁻⁶, relatively few studies are available for the
52 osteocytes since they are embedded inside the hard mineralized bone matrix, causing a
53 difficulty in accessibility to isolate the primary cells. Although the method of isolation and
54 cultivation of osteocytes has been recently reported⁷, it is still challenging to maintain the
55 osteocyte-likeness *in vitro*. As a surrogate of osteocyte, osteoblastic cells have been widely
56 utilized in many studies⁸.

57 While the osteocytes are captured in the mineralized bone matrix, they are subjected to hypoxic
58 condition in a narrow space because they reside distant from the blood vessels^{9,10}. Due to
59 practical reasons such as a difficulty in accessibility to the osteocytes *in vivo*, a physiological
60 level of oxygen concentration applied to the osteocytes has not been reported. However, several
61 studies have attempted to apply this hypoxic condition in order to figure out its effect on the
62 osteoblasts/osteocytes. The hypoxic condition using 1 or 5% O₂ concentration modulated the
63 transformation to osteocytes from osteoblasts¹¹ or *ORP150* expression levels in mouse

64 osteoblast-like MC3T3-E1 cells¹². As reported by those groups, we assumed that the hypoxia
65 plays a significant role in cellular differentiation capability for osteocytes.

66 Recently, application of three-dimensional (3D) scaffold-free tissue engineering techniques,
67 referred to as organoids, have been widely broadened in the field of fundamental biology,
68 particularly in human development, disease, or drug screening. Compared to a conventional
69 two-dimensional (2D) culture technique, the 3D culture system is regarded as a more
70 biomimetic tissue models by providing an appropriate cell-cell or cell-matrix interaction¹³.
71 While most of the fundamental biology on cellular behaviors or functions of osteocytes were
72 studied using the 2D culture system, we attempted to fabricate a novel 3D tissue engineered
73 osteocytic model and further to elucidate its response to hypoxia.

74

75 **Materials and method**

76 **Cell culture and hypoxia**

77 Mouse osteoblast-like cells, MC3T3-E1, were provided by RIKEN Cell Bank and cultured in
78 α -MEM (Gibco) containing 10% FBS (Gibco) and 1% antibiotic-antimycotic (Gibco) in a
79 humidified incubator at 37 °C with 5% CO₂. When the cells become 80 – 90 % confluent, a
80 cell passage was carried out. In this study, we applied a hypoxic condition to samples using a
81 BIONIX hypoxic culture kit (Sugiyama-gen). According to the manufacturer's manual, the
82 samples were subjected to hypoxia (5% O₂) for 48 hours during the fabrication process of SFT
83 (Day 0 – Day 2) or 2 days after the SFT was fabricated (Day 2 – Day 4).

84

85

86 **Fabrication of scaffold-free tissue**

87 In order to prepare for a scaffold-free tissue (SFT), the MC3T3-E1 cells were subcultured at a
88 cell density of 50,000 cells (1,300 cells/mm²) in a 7 mm diameter of glass ring which was set
89 on the culture dish as illustrated in Fig. 1(A). A monolayer of the cells was formed inside the
90 ring by culturing for 2 days. Then, 2,000,000 cells (51,995 cells/mm²) were subcultured on top
91 of the monolayer inside the ring. The monolayer embedded helped to retain the disk shape
92 inside the ring as described in the Fig. 1 (B). After 3 hours of incubation, the ring was gently
93 removed to provide sufficient nutrients to a 3D tissue-engineered construct, termed SFT. As
94 represented in Fig. 1(C) and (D), the SFT was further incubated for 2 days according to
95 experiments. For control sample, 200,000 cells (208 cells/mm²) were subcultured on a culture
96 dish to form a conventional 2D monolayer model reconstructed by MC3T3-E1 and incubated
97 to become fully confluent after 2 days of culture period in Fig. 1(E).

98

99 **Real-time PCR**

100 For RNA extraction, the samples were first washed once with PBS and collected with 1 ml of
101 Isogen II (Nippon Gene). After adding 50 µl of p-Bromoanisole (Nacalia Tesque), the tube was
102 vortexed thoroughly for 10 seconds and centrifuged at 12,000 g for 10 minutes at 4 °C.
103 Following centrifugation, the mixture was separated into two phases. A colorless upper
104 aqueous phase of the mixture was carefully transferred into a new microtube and mixed with
105 the same amount of 70% ethanol. After being vortexed, the mixture was transferred into the
106 spin cartridge (PureLink RNA Mini Kit; Invitrogen). According to the manufacturer's protocol,
107 the samples were then centrifuged, followed by washing process. The samples were then dried
108 and quickly added an appropriate amount of RNase free water. For cDNA synthesis and real-

109 time quantitative PCR, we utilized the Transcriptor Universal cDNA Master (Roche) and
110 PowerUp SYBR Green Master Mix (ThermoFisher), respectively. We then investigated runt
111 related transcription factor 2 (*Runx2*), alkaline phosphatase (*Alp*), and collagen, type I, alpha 1
112 chain (*Colla1*) as osteoblast markers while osteopontin (*Opn*), the phosphate regulating
113 endopeptidase homolog X-linked (*Phex*), the dentin matrix protein 1 (*Dmp1*), and sclerostin
114 (*Sost*) were utilized as osteocyte markers. As hypoxia-regulated markers, we also examined
115 hypoxia-inducible factor (*Hif1 α*) and erythropoietin (*Epo*). All the PCR primers were described
116 in Table 1 and classified as previous studies^{14,15}. All the gene expressions were normalized to
117 those of a reference gene, *Gapdh*.

118

119 **Immunostaining**

120 The SFT samples were washed twice with PBS and collected in the 4% paraformaldehyde
121 (PFA) at room temperature for 15 minutes. After flushing twice with PBS, the samples were
122 permeabilized using 0.1% triton X-100 at room temperature for 30 minutes. The samples were
123 then washed twice with PBS and treated with 4% bovine serum albumin (Sigma) in PBS at
124 room temperature for 1 hour to block non-specific interactions. After washing the blocking
125 reagent, it is treated with the primary antibody, anti-DMP1 antibody (Abcam), overnight at
126 4 °C. Then, the samples were washed twice with PBS and incubated with the Alexa Flour 546
127 secondary antibody (Invitrogen), Alexa Fluor 488 Phalloidin (Invitrogen), and DAPI (Sigma)
128 at room temperature for 1 hour. The stained samples were finally washed twice with PBS and
129 preserved in PBS until the time of observation. The samples were observed using the
130 FLUOVIEW FV3000 (Olympus).

131

132 **Statistical analysis**

133 The bars in the real-time PCR represent the mean \pm standard error values. A Student's t-test or
134 two-way ANOVA with Fisher's least significant difference (LSD) post hoc test (with $\alpha = 0.05$)
135 was carried out to evaluate the statistical difference. *P*-value of 0.05 or less was assumed to be
136 significant.

137

138 **Results**

139 **Osteoblast-like cells in three-dimensional scaffold-free tissue enhanced osteocyte**
140 **differentiation within 2 days**

141 The SFT and monolayer reconstructed by osteoblast-like cells were incubated for 2 days. Real-
142 time PCR analysis in Fig. 2 (A) showed that the osteoblast-like cells in the SFT had significant
143 reductions in *Runx2* (0.30-fold change; $p < 0.005$), *Alp* (0.28-fold change; $p < 0.05$), and
144 *Coll1a1* (0.12-fold change; $p < 0.005$), compared to that in the monolayer. On the other hand,
145 the SFT rendered remarkable up-regulations in the osteocyte mRNA expressions, such as *Opn*
146 (1.79-fold change; $p < 0.05$), *Phex* (4.00-fold change; $p < 0.05$), *Dmp1* (23.3-fold change; $p <$
147 0.05), and *Sost* (17.8-fold change; $p < 0.05$). To elucidate the spatial information on osteocyte
148 protein expression in the SFT, we conducted DMP1 immunostaining. DMP1 expression was
149 examined because *Dmp1* mRNA expression in the SFT measured by real-time PCR was most
150 up-regulated among the osteocyte markers. As described in Fig. 2 (B) – (E), the staining results
151 showed that the DMP1 expression (green) was entirely detected in the SFT. The staining
152 images also represented that the SFT had a thickness of about 50 μm .

153

154 **Hypoxia promoted *Sost* gene expression for osteoblast-like cells in the scaffold-free tissue**

155 In this experiment, we applied 5% hypoxic condition to monolayer and SFT for 48 hours during
156 fabrication period (Day 0 – Day 2). Then, we evaluated changes in mRNA expressions of
157 osteoblast and osteocyte markers in the absence or presence of hypoxia as shown in Fig. 3. By
158 applying hypoxia, it reduced *Runx2* (0.67-fold change) and *Coll1a1* (0.74-fold change) in the
159 monolayer while the hypoxia suppressed *Runx2* (0.36-fold change), *Alp* (0.40-fold change),
160 and *Coll1a1* (0.41-fold change) mRNA expressions in the SFT. Applying hypoxia in the
161 monolayer did not also alter the osteocyte mRNA expressions for 2 days; *Phex* (0.89-fold
162 change), *Dmp1* (0.92-fold change), and *Sost* (1.15-fold change). On the other hand, the hypoxia
163 significantly up-regulated *Sost* (2.46-fold change) mRNA expression in the SFT while *Phex*
164 (0.96-fold change) and *Dmp1* (0.78-fold change) mRNA expressions were not modulated in
165 the SFT. Furthermore, we also investigated *Hif1 α* and *Epo* mRNA expression as hypoxia-
166 related markers. The hypoxia significantly altered *Hif1 α* (0.60-fold change) and *Epo* mRNA
167 expressions (2.38-fold change) in the monolayer while it also greatly modulated *Hif1 α* (0.36-
168 fold change) and *Epo* mRNA expressions (6.74-fold change) in the SFT.

169

170 **Hypoxia maintained up-regulation of *Sost* gene expression for osteoblast-like cells in the**
171 **scaffold-free tissue**

172 To investigate the effect of hypoxia after fabrication of SFT for maintenance of osteocyte
173 differentiation, we conducted a hypoxic experiment between Day 2 and Day 4. In Fig. 4,
174 applying hypoxia to the monolayer reconstructed by osteoblast-like cells significantly down-
175 regulated all the mRNA expressions of osteoblast markers such as *Runx2* (0.39-fold change),
176 *Alp* (0.52-fold change), and *Coll1a1* (0.40-fold change), while the hypoxia also reduced the

177 *Runx2* (0.34-fold change), *Alp* (0.18-fold change), and *Coll1a1* (0.30-fold change) mRNA
178 expressions in the SFT. On the other hand, in the monolayer, the hypoxia non-significantly
179 down-regulated the osteocyte gene expression; *Phex* (0.44-fold change), *Dmp1* (0.43-fold
180 change), and *Sost* (0.28-fold change). Regarding the SFT, the hypoxia did not alter the
181 osteocyte mRNA expression; *Phex* (0.88-fold change), *Dmp1* (0.89-fold change), and *Sost*
182 (1.79-fold change). Those results indicate that applying the hypoxia maintained the osteocyte
183 markers in the SFT. Moreover, we also examined the hypoxia-induced genes. The hypoxia
184 modulated *Hif1 α* (0.46-fold change) and *Epo* mRNA expressions (0.56-fold change) in the
185 monolayer, whereas it altered *Hif1 α* (0.44-fold change) and *Epo* mRNA expressions (1.25-fold
186 change) in the SFT.

187

188 **Discussion**

189 While three-dimensional (3D) *in vitro* model such as organoids have become a powerful tool
190 in the fundamental biological research, our group showed that osteoblast cells in the form of
191 3D spheroid structure triggered the osteocyte differentiation^{16,17}. In this study, we developed a
192 novel disk type of 3D *in vitro* model, referred to as scaffold-free tissue (SFT), and further
193 investigated the capability of osteocyte differentiation for osteoblast-like cells in the form of
194 SFT compared to the 2D monolayer condition. In Fig. 2 (A), the osteocyte markers (*Opn*, *Phex*,
195 *Dmp1*, and *Sost*) were highly up-regulated in the SFT after 2 days of cultivation while it
196 suppressed the osteoblast mRNA expressions (*Runx2*, *Alp*, and *Coll1*). Moreover, the
197 expression level of an osteocytic protein, DMP1, was detected entirely inside the SFT. Similar
198 to the previous studies^{16,17}, we showed that the osteoblast-like cells in the 3D culture system of

199 SFT exerted the osteocyte-likeness within 2 days, in the absence of chemical induction such as
200 osteogenic supplements.

201 In this study, we also examined the effect of hypoxia regarding changes in gene expression
202 levels of osteocyte differentiation markers. Since the osteocytes were embedded in the
203 mineralized bone, the osteocytes *in vivo* are thought to be subjected to the hypoxic condition.
204 Based on other reported study¹¹, we applied 5% hypoxia to the monolayer and SFT
205 reconstructed by osteoblast-like cells during fabrication of the SFT (Day 0 – 2). As a result of
206 applying hypoxic condition to the samples, the hypoxia-related genes, such as *Hif1a* and *Epo*,
207 were significantly altered as shown in Fig. 3. Our results regarding decrease in *Hif1a* and
208 increase in *Epo* genes under hypoxic condition correspond to other studies using the
209 conventional 2D model^{18,19}. Particularly, we first represented that those hypoxia-related genes
210 were also modulated in the 3D SFT under hypoxia. In the monolayer condition, the hypoxia
211 suppressed osteoblast gene expressions within 2 days while there is no significant change in
212 osteocyte gene expressions as shown in Fig. 3. In the SFT, however, the hypoxia significantly
213 up-regulated *Sost* mRNA expression, whereas the *Sost* mRNA expression was not altered in
214 the monolayer. As the *Sost* gene is regarded as a matured osteocyte marker¹⁴, the result may
215 indicate that the hypoxic condition in the 3D SFT culture system enhance the initiation of
216 osteocyte differentiation. Despite the up-regulation of *Sost* gene expression in the SFT under
217 hypoxia, further detailed study regarding the osteocyte differentiation need to be undertaken.

218 To examine the effect of hypoxia after the fabrication of SFT for maintenance of osteocyte
219 differentiation, we also applied the hypoxia on Day 2 for 48 hours (Day 2 – 4) and then
220 conducted real-time PCR in Fig 4. Similar to the result in Fig. 3, the hypoxia significantly
221 down-regulated all the osteoblast mRNA expressions in both monolayer and SFT. Regarding
222 with the osteocyte markers, the hypoxia non-significantly reduced *Phex*, *Dmpl*, and *Sost* gene

223 expressions in the monolayer, whereas those markers in the SFT were retained by the hypoxia.
224 Hence, we hereby first reported the different manner of *Sost* gene expressions response to
225 hypoxia in the 3D SFT compared to the conventional 2D monolayer condition. We, however,
226 did not evaluate the effect of different oxygen tensions or its duration, so that the effect of
227 various hypoxic condition on the osteocyte differentiation needs to be further studied in the
228 future.

229 While little is known about the hypoxic effect on the osteocyte differentiation *in vitro*, our
230 findings are meaningful because the hypoxia may modulate the initiation and maintenance of
231 osteocyte differentiation in the 3D SFT. Although it is still unclear why the 3D SFT had a
232 response to hypoxia in a different manner compared to the 2D monolayer, these results
233 suggested an importance and requirement of 3D *in vitro* model for fundamental biological
234 research, whereas the conventional 2D model may not fully recapitulate the *in vivo* situation.
235 Since the maintenance of osteocyte-likeness *in vitro* for osteocyte research is still challenging,
236 our 3D model as well as recruitment of hypoxic culture condition has a potential to be utilized
237 as a new *in vitro* culture strategy for the osteocyte.

238 In this present study, we successfully established a fabrication method of SFT reconstructed
239 by mouse osteoblast-like cells based on Furukawa's study²⁰. Particularly, the SFT in this study
240 was fabricated by embedding a cell monolayer underneath the SFT to fix it as described in Fig.
241 1(A) and (B). Without the monolayer, the SFT was not able to retain its shape as desired and
242 eventually become shrunken due to their strong cell contraction forces in Fig.1 (B). By using
243 this monolayer embedded underneath, we successfully fabricated the SFT on the culture dish.
244 The SFT is a thick tissue-engineered construct with a thickness of about 50 μm , compared to a
245 conventional cell sheet with a thickness of 20 μm ²¹.

246 The SFT developed in this study is also thought to be suitable for *in vivo* study by
247 transplantation for bone regeneration because it is a thicker 3D tissue engineered construct than
248 the conventional cell sheet model²². The present method allowed to make it possible to detach
249 the SFT from the normal culture dish by mechanically scrapping it, without recruiting a
250 temperature-responsive culture dish. Since the temperature-responsive culture dish is an
251 essential experimental tool in the conventional cell-sheet technologies^{23,24}, our novel method
252 did not recruit a specific culture dish to fabricate the SFT. While most of the studies in the bone
253 tissue engineering have utilized a scaffold-based technology for several decades²⁵, the scaffold
254 is derived from artificial materials which have a risk to cause the foreign body reaction after
255 transplantation. On the other hand, the SFT model does not recruit any artificial materials, but
256 only cells. Hence, the *in vivo* study transplanting the SFT will be expected to become an
257 alternative in the field of tissue engineering for clinical applications.

258 In conclusion, we successfully established the method to fabricate the SFT reconstructed by
259 mouse osteoblast-like cells. We showed that the osteoblast-like cells in the form of the SFT
260 rendered the osteocyte-likeness within 2 days. Moreover, we first attempted to utilize the 3D
261 SFT, as a new *in vitro* osteocytic model, in response to hypoxia. Our present study suggested
262 that the hypoxia may be required to promote the initiation of osteocyte differentiation and also
263 to maintain the osteocyte differentiation for the osteoblast-like cells *in vivo* situation. Most
264 interestingly, our finding highlighted the potential significance of 3D *in vitro* model to mimic
265 the *in vivo* situation.

266

267 **Acknowledgement**

268 We would like to appreciate Junko Sunaga for providing technical advices. This work was
269 supported by the Japan Society for the Promotion of Science (JSPS) KAKENHI (19K23604,
270 20K20181, and 20H00659), Advanced Research and Development Programs for Medical
271 Innovation (AMED-CREST), by elucidation of mechanobiological mechanisms and their
272 application to the development of innovative medical instruments and technologies from Japan
273 Agency for Medical Research and Development (AMED) (JP20gm0810003), and by the
274 acceleration program for intractable diseases research utilizing disease-specific iPS cells from
275 AMED (JP19bm0804006).

276

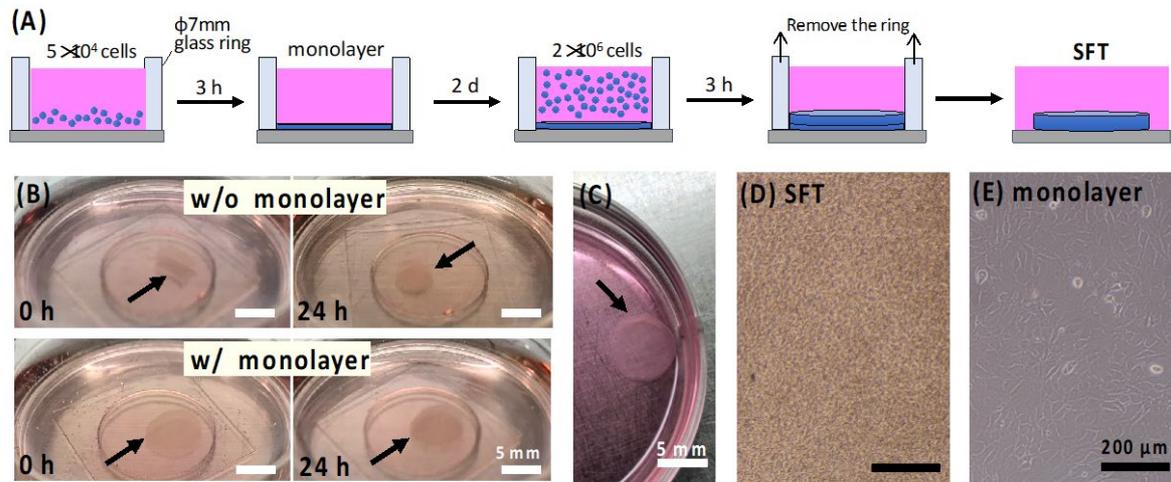
277 **References**

- 278 1. Adachi, T., Aonuma, Y., Ito, S., Tanaka, M., Hojo, M., Takano-Yamamoto, T., et al.
279 Osteocyte calcium signaling response to bone matrix deformation. *J Biomech.* **42**,
280 2507, 2009.
- 281 2. Robling, A.G., and Bonewald, L.F. The Osteocyte : New Insights. *Annu Rev Physiol.*
282 **82**, 485, 2020.
- 283 3. Kawanishi, M., Oura, A., Furukawa, K., Fukubayashi, T., Nakamura, K., Tateishi, T.,
284 et al. Redifferentiation of dedifferentiated bovine articular chondrocytes enhanced by
285 cyclic hydrostatic pressure under a gas-controlled system. *Tissue Eng.* **13**, 957, 2007
- 286 4. Kim, J., Montagne, K., Nemoto, H., Ushida, T., and Furukawa, K.S. Hypergravity
287 down-regulates c-fos gene expression via ROCK/Rho-GTP and the PI3K signaling
288 pathway in murine ATDC5 chondroprogenitor cells. *PLoS One.* **12**, e0185394, 2017.

- 289 5. Fahy, N., Alini, M., and Stoddart, M.J. Mechanical stimulation of mesenchymal stem
290 cells: Implications for cartilage tissue engineering. *J Orthop Res.* **36**, 52, 2018.
- 291 6. Kim, J., Ushida, T., Montagne, K., Hirota, Y., Yoshino, O., Hiraoka, T., et al.
292 Acquired contractile ability in human endometrial stromal cells by passive loading of
293 cyclic tensile stretch. *Sci Rep.* **10**, 9014, 2020.
- 294 7. Shah, K.M., Stern, M.M., Stern, A.R., Pathak, J.L., Bravenboer, N., and Bakker, A.D.
295 Osteocyte isolation and culture methods. *Bonekey Rep.* **5**, 838, 2016.
- 296 8. Boukhechba, F., Balaguer, T., Michiels, J.F., Ackermann, K., Quincey, D., Bouler,
297 J.M., et al. Human primary osteocyte differentiation in a 3D culture system. *J Bone*
298 *Miner Res.* **24**, 1927, 2009.
- 299 9. Dodd, J.S., Raleigh, J.A., and Gross, T.S. Osteocyte hypoxia: A novel
300 mechanotransduction pathway. *Am J Physiol.* **277**, 598, 1999.
- 301 10. Schipani, E., Ryan, H.E., Didrickson, S., Kobayashi, T., Knight, M., and Johnson, R.S.
302 Hypoxia in cartilage: HIF-1 α is essential for chondrocyte growth arrest and survival.
303 *Genes Dev.* **15**, 2865, 2001.
- 304 11. Hirao, M., Hashimoto, J., Yamasaki, N., Ando, W., Tsuboi, H., Myoui, A., et al.
305 Oxygen tension is an important mediator of the transformation of osteoblasts to
306 osteocytes. *J Bone Miner Metab.* **25**, 266, 2007.
- 307 12. Montesi, M., Jähn, K., Bonewald, L., Stea, S., Bordini, B., and Beraudi, A. Hypoxia
308 mediates osteocyte ORP150 expression and cell death in vitro. *Mol Med Rep.* **14**,
309 4258, 2016.

- 310 13. Nam, K.H., Smith, A.S.T., Lone, S., Kwon, S., and Kim, D.H. Biomimetic 3D Tissue
311 Models for Advanced High-Throughput Drug Screening. *J. Lab. Autom.* **20**, 201,
312 2015.
- 313 14. Bonewald, L.F. The amazing osteocyte. *J Bone Miner Res.* **26**, 229, 2011.
- 314 15. Capulli, M., Paone, R., and Rucci, N. Osteoblast and osteocyte: Games without
315 frontiers. *Arch. Biochem. Biophys.* **561**, 3, 2014.
- 316 16. Kim, J., and Adachi, T. Cell Condensation Triggers the Differentiation of Osteoblast
317 Precursor Cells to Osteocyte-Like Cells. *Front Bioeng Biotechnol.* **7**, 2019.
- 318 17. Kim, J., Kigami, H., and Adachi, T. Characterization of self-organized osteocytic
319 spheroids using mouse osteoblast-like cells. *J Biomech Sci Eng.* **15**, 20-00227, 2020.
- 320 18. Janaszak-Jasiecka, A., Bartoszewska, S., Kochan, K., Piotrowski, A., Kalinowski, L.,
321 Kamysz, W., et al. MiR-429 regulates the transition between Hypoxia-Inducible Factor
322 (HIF)1A and HIF3A expression in human endothelial cells. *Sci Rep.* **6**, 22775, 2016.
- 323 19. Stockmann, C., and Fandrey, J. Hypoxia-induced erythropoietin production: A
324 paradigm for oxygen-regulated gene expression. *Clin. Exp. Pharmacol. Physiol.* **33**,
325 968, 2006.
- 326 20. Furukawa, K.S., Imura, K., Tateishi, T., and Ushida, T. Scaffold-free cartilage by
327 rotational culture for tissue engineering. *J Biotechnol.* **133**, 134, 2008.
- 328 21. Miyahara, Y., Nagaya, N., Kataoka, M., Yanagawa, B., Tanaka, K., Hao, H., et al.
329 Monolayered mesenchymal stem cells repair scarred myocardium after myocardial
330 infarction. *Nat Med.* **12**, 459, 2006.

- 331 22. Sumide, T., Nishida, K., Yamato, M., Ide, T., Hayashida, Y., Watanabe, K., et al.
332 Functional human corneal endothelial cell sheets harvested from temperature-
333 responsive culture surfaces. *FASEB J.* **20**, 392, 2006.
- 334 23. Yang, J., Yamato, M., Kohno, C., Nishimoto, A., Sekine, H., Fukai, F., et al. Cell sheet
335 engineering: Recreating tissues without biodegradable scaffolds. *Biomaterials.* **26**,
336 6415, 2005.
- 337 24. Matsuda, N., Shimizu, T., Yamato, M., and Okano, T. Tissue engineering based on
338 cell sheet technology. *Adv Mater.* **19**, 3089, 2007.
- 339 25. Du, Y., Guo, J.L., Wang, J., Mikos, A.G., and Zhang, S. Hierarchically designed bone
340 scaffolds: From internal cues to external stimuli. *Biomaterials.* **218**, 119334, 2019.
- 341
- 342



343

344

345 Figure 1. Fabrication of scaffold-free osteocytic tissue. (A) Schematic diagram illustrating the

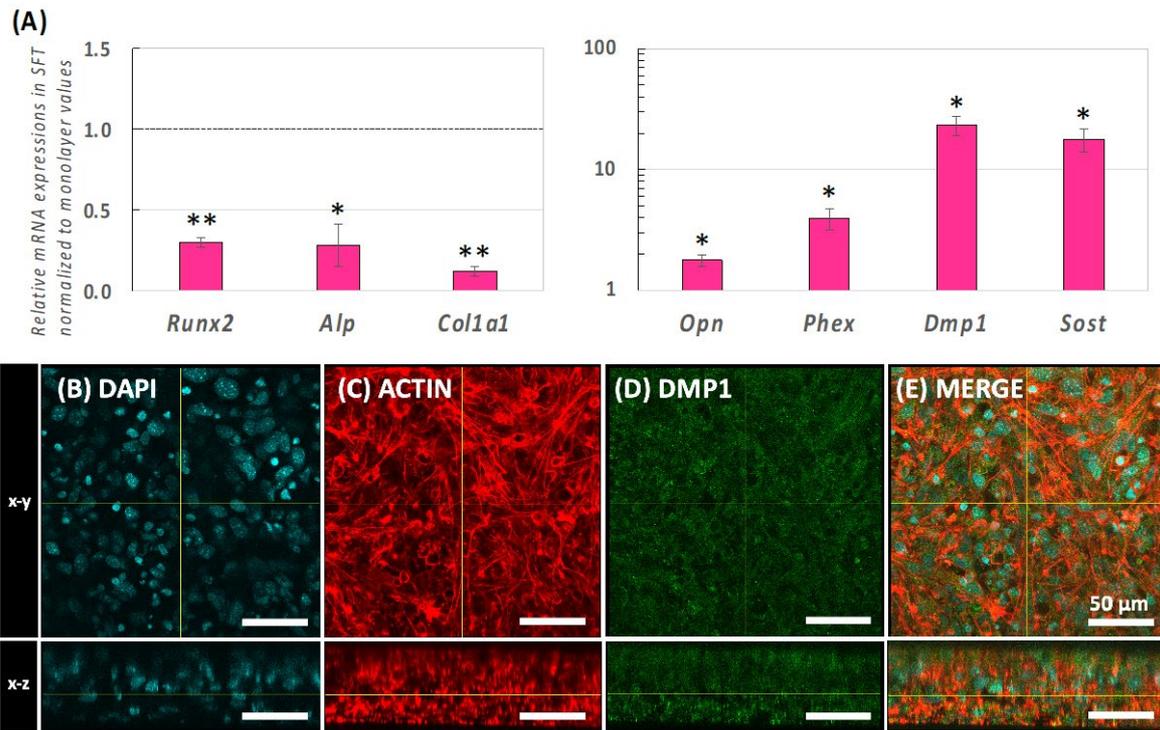
346 fabrication method for scaffold-free tissue (SFT) reconstructed by mouse osteoblast-like cells.

347 (B) Images of SFT with or without a monolayer embedded underneath the SFT immediate or

348 24 hours after removing a glass ring. (C) Image of the SFT after 2-day incubation. Microscope

349 image of (D) scaffold-free tissue and (E) monolayer reconstructed by osteoblast-like cells.

350

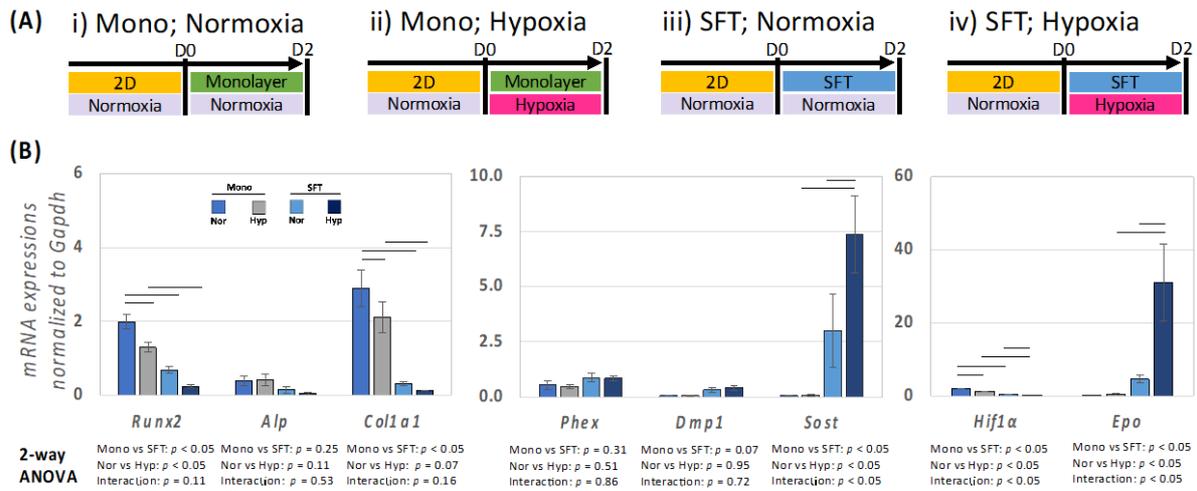


351

352

353 Figure 2. Induced osteocytogenesis in the SFT after 2-day incubation. (A) Real-time PCR
 354 analysis of relative mRNA expression of osteoblast markers (*Runx2*, *Alp*, and *Colla1*) and
 355 osteocyte marker (*Opn*, *Phex*, *Dmp1*, and *Sost*) after 2-day incubation. Graphs represent the
 356 relative mRNA expression levels in the SFT normalized to *Gapdh* mRNA expression levels
 357 and further normalized to monolayer values. The relative mRNA expressions in the SFT were
 358 then normalized to that in the monolayer. The bars indicate the mean \pm standard error ($n = 7$;
 359 p -value was obtained from Student's t-test; * $p < 0.05$, ** $p < 0.005$). Immunostaining images
 360 of the scaffold-free tissue, 2-day incubation; (B) DAPI; (C) F-ACTIN; (D) DMP1; (E) MERGE.

361



362

363

364 Figure 3. Up-regulation of *Sost* gene expression in the SFT under hypoxia during the

365 fabrication period (Day 0 – 2). (A) Schematic overview of hypoxic experiment for the SFT.

366 (B) The mRNA expression in the monolayer and SFT after applying 5% hypoxia for 48 hours

367 during the fabrication period (Day 0 – 2). Osteoblast (*Runx2*, *Alp*, and *Colla1*), osteocyte (*Opn*,

368 *Phex*, *Dmp1*, and *Sost*), and hypoxia-induced markers (*Hif1α* and *Epo*) in the monolayer and

369 SFT were measured by real-time PCR, in the absence and presence of hypoxia. The graphs

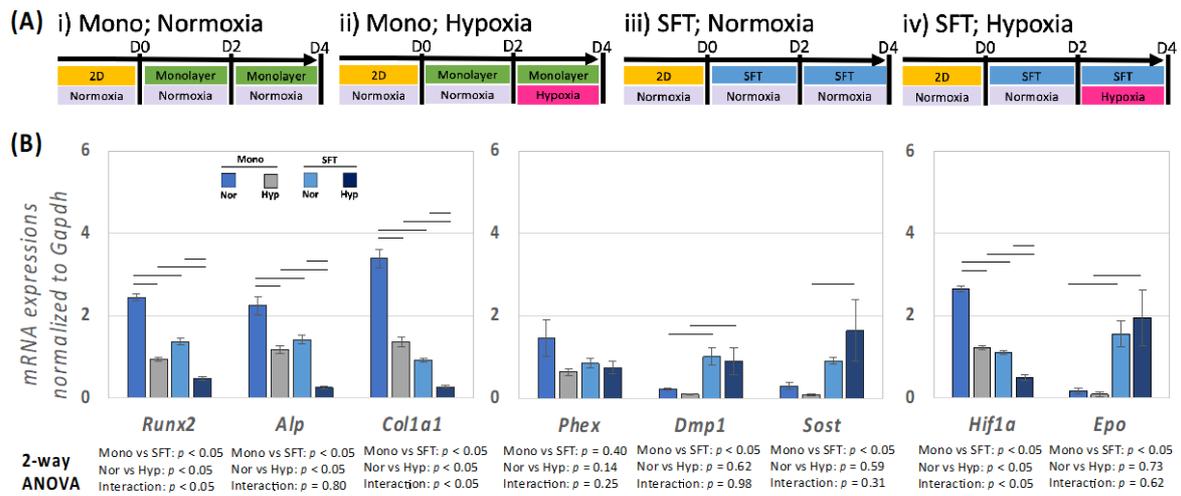
370 represent the mRNA expression levels normalized to *Gapdh* mRNA expression levels. The

371 colored bars indicate the mean \pm standard error ($n = 6$; bar indicates the significance between

372 the graphs, which was obtained from two-way ANOVA and Fisher's LSD post hoc test; $\alpha =$

373 0.05).

374



375

376

377 Figure 4. Maintained osteocyte gene expressions in the SFT under hypoxia after the fabrication

378 period (Day 2 – 4). (A) Schematic overview of hypoxic experiment for the SFT. (B) The

379 mRNA expression in the monolayer and SFT being subjected to hypoxic condition for 48 hours

380 after the fabrication period (Day 2 – 4). Osteoblast (*Runx2*, *Alp*, and *Colla1*), osteocyte (*Opn*,

381 *Phex*, *Dmp1*, and *Sost*), and hypoxia-induced markers (*Hif1a* and *Epo*) in the monolayer and

382 SFT were measured by real-time PCR, in the absence and presence of hypoxia. The graphs

383 represent the mRNA expression levels normalized to *Gapdh* mRNA expression levels. The

384 colored bars indicate the mean \pm standard error ($n = 6$; bar indicates the significance between

385 the graphs, which was obtained from two-way ANOVA and Fisher's LSD post hoc test; $\alpha =$

386 0.05).

387

388 Table 1. Primer List

Gene	Forward primer	Reverse primer	Amplicon size (bp)
<i>Gapdh</i>	TGTTCCCTACCCCAATGTGT	GGTCCTCAGTGTAGCCCAAG	137
<i>Runx2</i>	CAGTCCCAACTTCCTGTGCT	TACCTCTCCGAGGGCTACAA	94
<i>Alp</i>	GCTGATCATTCACGTTTT	ACCATATAGGATGGCCGTGA	120
<i>Col1a1</i>	CGTGCAATGCAATGAAGAAC	TCCCTCGACTCCTACATCTTCT	118
<i>Opn</i>	CCCGGTGAAAGTGACTGATT	GGCTTTCATTGGAATTGCTT	191
<i>Phex</i>	AGGCATCACATTCACCAACA	ATGGCACCATTGACCCTAAA	103
<i>Dmp1</i>	GGTTTTGACCTTGTGGGAAA	AATCACCCGTCCTCTCTTCA	91
<i>Sost</i>	CGTGCCTCATCTGCCTACTT	ATAGGGATGGTGGGGAGGT	185
<i>Hif1α</i>	GGCGACACCATCATCTCTCT	TTTGGAGTTTCCGATGAAGG	164
<i>Epo</i>	CCACCCTGCTGCTTTTACTC	GACCTTCTGCACAACCCATC	156

389